Development and evaluation of a passive acoustic localization method to monitor fish spawning aggregations and measure source levels

Katherine C. Wilson
Scripps Institution of Oceanography
University of California
San Diego, CA, USA
katherine.c.wilson11@gmail.com

Brice X. Semmens
Scripps Institution of Oceanography
University of California
San Diego, CA, USA
bsemmens@ucsd.edu

Stephen R. Gittings
Office of National Marine Sanctuaries
NOAA
Silver Spring, MD, USA
steve.gittings@noaa.gov

Christy Pattengill-Semmens
Reef Environmental Education Foundation
Key Largo, FL, USA
christy@reef.org

Ana Širović
Scripps Institution of Oceanography &
Texas A&M University
Galveston, TX, USA
asirovic@tamug.edu

***Abstract*— More than 800 species of fish produce sound including red hind (*Epinephelus guttatus*), Nassau (*E. striatus*), black (*Mycteroperca bonaci*), and yellowfin grouper (*M. venenosa*). Their sounds can be used to monitor these fish and may be a means to estimate abundance if parameters such as source levels, detection probabilities, and cue rates are known. During the week of Nassau grouper spawning in February 2017, a passive acoustic array was deployed off Little Cayman Island to study the temporal and spatial dynamics of spawning aggregations of Nassau grouper and red hind and measure the source levels of the sounds produced by all four species. The localization method was based on hyperbolic localization of cross-correlated time differences of arrival and its accuracy evaluated via simulations and empirical measurements. The mean peak-to-peak source levels ranged from 143.7 dB for yellowfin grouper to 152.0 dB for Nassau grouper (re: 1µPa at 1m for 70 to 170 Hz) with an estimated error of 2 to 10 dB based on the localization error results (the mean localization error for empirical measurements was 3.3 ± 3.8 m and errors in simulations ranged from 1.1 ± 1.7 to 16.6 ± 0.9 m for inside the array). The source level error due to localization was comparable to the measured variances for source levels. This and the high number of localizations at fish spawning aggregations suggests that localization can be used to accurately measure source levels, detection ranges, and other variables needed for density estimation of spawning aggregations.**

Keywords—passive acoustics, source levels, localization, grouper, fish spawning aggregations

I. Introduction

Passive acoustic monitoring (PAM) provides a means to observe sound-producing animals, including the more than 800 species of fish that produce sound related to spawning, aggression, and/or disturbance. Groupers, a common name for many of the fish within the family Epinephelidae, are economically important fish globally and many species are known to produce sound [1]. Population estimation methods for groupers have been limited to underwater visual census or catch per unit effort for aggregated fish [2]. Globally, grouper management and policy is largely based on fishing reports or data that are temporally and spatially limited. However, development of density estimates based on sound production can provide another means for estimating abundance. Also, observations of grouper populations have often been limited in time or space due to limitations of common methods such as SCUBA, trawls, acoustic telemetry, reported landings or catches, etc., to observe marine fish. Passive acoustic localization can be used to provide continuous spatiotemporal information about sound-producing fishes and obtain variables needed for passive acoustic density estimation, but the accuracy of these observations or variables depends on the performance of the localization method.

Passive acoustic localization has commonly been used in marine mammal studies [3]-[6] but it has been more rare for fishes [8] due to challenges related to fish sound propagation: shallow-water environments and smaller propagation range of sounds. Additionally, there have been relatively few studies to measure fish source levels [8]-[15] or investigate the relation between sound levels and fish abundance [16], [17]. However, the results of [16] and [17], suggest that passive acoustic density estimation methods like the ones used for marine mammals [3], [18], and [19] could be developed for some fishes. In those cases, by localizing on calling animals, it may be possible to measure the variables needed for these estimates, including source levels [8].

Time-difference-of-arrival (TDOA) localization error can be evaluated using ground-truth measurements, or more commonly, using simulations. The Cramer Rao Lower Bound (CRLB) is a metric that is commonly used to determine the minimum achievable error for tracking systems. For time-of-arrival measurements, the CRLB is dependent of the bandwidth

Research was supported by NSF CNS INSPIRE grant #1344291 and DoD, Air Force Office of Scientific Research via the NDSEG Fellowship, 32 CFR 168a.

of the signal and the signal-to-noise ratio (SNR) at the receivers [20]. Many other factors can contribute to error in the position estimates in addition to the TDOA measurements. Some of these factors include: uncertainty in receiver positions, environmental properties (sound speed, bottom type, etc.) and propagation effects [21]; acoustic properties of the signal [22]; the number of arrivals used for localization [21]; SNR of these arrivals [23]; impulsive noise leading to anomalous errors in TDOA measurements [24]; and the presence of other signals [25]. Simulations that model all of the possible error sources help with assessing the limitations of the localization performance.

A localization method was developed and tested at a Nassau grouper (*Epinephelus striatus)* spawning aggregation. Nassau grouper is an endangered species that forms fish spawning aggregations where hundreds to thousands of fish gather annually at one location for approximately a week in one or two consecutive months for spawning. One of the largest known remaining spawning aggregations of Nassau grouper forms off Little Cayman, Cayman Islands. Nassau grouper is known to produce three call types [26], [27] and sound production is common during aggregations. A variety of other grouper species also form spawn aggregations at this location and are known sound producers, including red hind (*Epinephelus guttatus*), black grouper (*Mycteroperca bonaci)*, and yellowfin grouper (*Mycteroperca venenosa*) [28]-[30]. Passive acoustics can be used to provide continuous observation to study these species off Little Cayman. The high density of fish and fish sound production during the spawning season of Nassau grouper at this location creates a good environment to evaluate the potential of passive acoustic localization methods for 1) in-situ measurements of sounds source levels and other variables needed for density estimation and 2) monitoring of aggregations and sound producing fishes.

To accomplish this, a passive acoustic array was deployed during the week of Nassau grouper spawning, February 11-19, 2017. 2D hyperbolic localization was developed to track the sounds produced by these four grouper species and measure their source levels in Little Cayman.

II. Methods

A. Data collection

A six-receiver passive acoustic array was deployed off the west end of Little Cayman (Fig. 1A) at a fish spawning aggregation (FSA) from February 11 to 19, 2017. It collected data continuously at a sample rate of 48 kHz. The array was constructed of three calibrated two-channel Wildlife Acoustics SM3M hydrophone recorders, each equipped with HTI-96 min hydrophones (-165 dB re: 1VμPa^{-1} from 20 Hz to 30 kHz), attached with 1 and 30 m cables. The hydrophones were deployed 0.5 to 1 m above the bottom at depths between 24 to 33 m with 18 to 40 m spacing between hydrophones (Fig. 1A). A 12 kHz source producing 2 ms pings approximately every 10 s was placed at the center of the array for the duration of the deployment to enable synchronization of the data.

Distances between receivers along the perimeter of the array, D_{ij}, and between each receiver and the 12 kHz pinger, D_i, were measured by SCUBA divers (Fig. 1B). These measurements were used to reconstruct the geometry of the array and solve for the positions, r, of a set of n receivers using a set of non-linear equations (1) and the Levenberg-Marquardt (LM) algorithm for least-squares error (LSE).

$$\min_{r\in\Re} \sum_{i=1}^{n} D_i - \sqrt{\sum(r_i - r_j)^2} \quad j = \begin{cases} i+1, & i<n \\ i, & i=n \end{cases} \qquad (1)$$

The bathymetry within the array (Fig. 1B) was estimated using video data collected from the location and the depth measurements at each receiver location. A SCUBA diver collected imagery of the entire array habitat using a Sony 4K video camera by swimming adjacent, overlapping transects while approximately maintaining a constant depth. Agisoft Metashape was used to stitch the video from each transect and develop a relative 3D map of the habitat, in which depth estimates were made based on the known receiver depths.

Additional data were collected during the deployment to evaluate localization error. Empirical measurements were collected at 15 known locations by placing a source that produced 2 ms, 22 kHz tones at an approximate 2 s period for 30 s or longer. These locations were along azimuths between each receiver and the center site at: 5 m inside the array perimeter, at the receivers, and, for odd numbered receivers, 5 and 10 m outside the perimeter (Fig. 1B).

B. 2D TDOA localization

Time-difference-of-arrival (TDOA) hyperbolic localization [21] was implemented with the Optimization Toolbox in MATLAB for 2D localization. The sound speed, c, was calculated for the area using regional models of sea surface

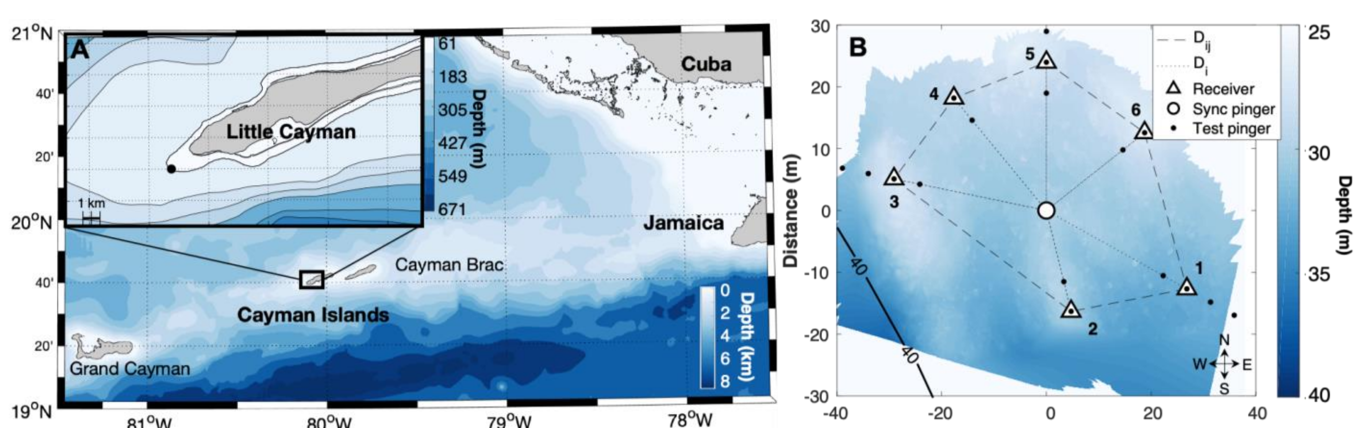

Fig. 1. Map of Little Cayman, Cayman Islands and the passive acoustic array. A) The Cayman Islands with the location of the array off the west end of Little Cayman shown in the inset. B) Each receiver location (triangles) is shown with the location of the 12 kHz pinger used for synchronization (white circle), diver measurements of the array (dashed lines), the locations of the 22 kHz pinger used for estimating localization error (black circles), and the bathymetry at the array location (colormap). The array was located close to the shelf break and the 40 m depth contour is shown to indicate the orientation of the break.

temperature (NOAA daily OISST [31]) and salinity (HYCOM [32]) and the Gibbs SeaWater Oceanographic Toolbox TEOS-10 for MATLAB [33]. Temperature measurements collected by divers during deployment and recovery were constant throughout the water column thus the sound speed was modeled as homogenous.

Manually identifying the start and end times of a signal of interest (a simulated signal, a ping, or a grouper sound) on a single receiver was the first step of the localization process. Next, the identified signal, referred to as the reference arrival (*RA*), was extracted and applied as a match filter [20], [34] to a segment of data from each of the other receivers. The maximum physical TDOAs, τ_{ijmax}, between the reference receiver and the other receivers were calculated and the start and end times of the *RA* were offset by τ_{ijmax} to determine the segment of data to extract from the other receivers. If the maximum output of the match filter was above an empirically determined threshold (Table 1) and the time lag of this maximum was within the range of $\pm \tau_{ijmax}$, a usable signal arrival was marked and the time lag was set to the TDOA between the *RA* and the arrival on the other receiver.

Signal-to-noise ratios (SNR) were calculated for the *RA* and the other usable arrivals and only arrivals with SNR greater than 3 dB were retained for localization. Power was calculated for a 0.2 s running window across the entire signal segment for a specific signal and noise bands (Table 1). This power was defined as the maximum value for each respective band. The bands were selected based on prior measurements of the signals of interest [26]-[30], [35] and the impulse response of the FIR bandpass filters used for each band. If three or more arrivals met these criteria, the TDOAs of every pair of arrivals was measured using cross-correlation and 2D hyperbolic localization was applied.

The LM algorithm was used to find the position, *s*, that minimized the LSE for the set of non-linear equations derived from the receiver positions, *r*, and *n* retained TDOAs, τ_{ij}, (2) producing the estimated position of the sound source. Due to instabilities in the algorithm found during simulations, which could lead to erroneous estimates, the algorithm was solved using 13 different initial starting points: the center pinger site, each receiver site, and positions 5 m outside the array perimeter at each receiver. The position estimate with the lowest LSE was used as the location of the sound source.

$$\min_{s \in \mathbb{R}^2} \sum_{i=1}^{n} \sum_{j=i+1}^{n} \frac{\sqrt{\sum (r_i - s)^2} - \sqrt{\sum (r_j - s)^2}}{c} - \tau_{ij} \quad (2)$$

Due to variable or impulsive background noise in many of the received arrivals, another step was required to constrain localization error. If there were more than three usable arrivals, the *RA* and the two arrivals with the strongest correlations were used to find an initial estimate of the source position first. Then, additional pairs of TDOA were individually added to the set of non-linear equations and a new position was estimated each time. All TDOA that produced a position estimate within a 2 m radius of the initial estimate were used to construct the final set of equations used for solving for position.

TABLE I. LOCALIZATION PARAMETERS. For each species listed in the first column, the threshold used to determine a signal arrival for matching filtering is shown (Match filter threshold). Additionally, the signal and noise bandwidths that were used for measuring the power of each for signal-to-noise ratios are shown in the last two columns, respectively (Signal BW and Noise BW).

Species	**Match filter threshold**	**Signal BW (Hz)**	**Noise BW (Hz)**
Nassau	0.2	75 – 250	300 - 475
Red hind	0.15	50 - 250	300 - 500
Black	0.4	50 - 225	300 - 475
Yellowfin	0.2	75 - 250	300 - 475

C. Error Simulations and analysis

Three simulations were conducted to model the error resulting from the localization method. These simulations were performed to evaluate error from 1) the LM algorithm and array geometry, 2) TDOA measurements, and 3) noise. The first two were conducted by simulating TDOAs only while the third simulated a test signal designed to have a frequency and bandwidth similar to the grouper sounds.

For the first simulation, the TDOA between each pair of receivers was calculated for a source located at all the positions over a 3D, 1 m gridded volume that spanned an 80 m by 80 m area across the array from 0 to 40 m depth. The delays for each assumed source location for all simulations were calculated using the homogenous sound speed of 1541.8 ms^{-1}. These calculated 3D TDOAs were input to LM algorithm to estimate 2D positions. The position error for all simulations and the empirical data was calculated as the 2D Euclidean distance between the simulated or known position and estimated 2D position.

In the second simulation, theoretical TDOAs were calculated for a 2D, 5 m gridded area that spanned the same 80 m by 80 m area across the array. Randomly assigned measurement errors were added to the 15 pairs of theoretical TDOAs for each position to simulate variable error in TDOA measurements. Two different limits for the measurement error that represented the range in time resolution, *T*, expected for the cross-correlation of the grouper calls were used: ± 0.014 and 0.004 s. They were estimated as an approximation of the CRLB using a common bandwidth and duration for grouper calls, 70 Hz and 1 to 3 s. For each simulated position, 1000 trials were run and the 95th percentile of the results was used as the position error.

The final simulation used a test signal representative of grouper sounds, in varying levels of noise, and TDOA error to simulate a more realistic scenario. The test signal was constructed from 1 s of white Gaussian noise (WGN) bandpass filtered from 75 to 125 Hz with a root-mean-square (RMS) power of 13.2 dB. An additional 1 s of 0 dB WGN was proportionately added before and after the signal to simulate theoretical TDOAs with error at each receiver. A maximum of ±1.7 ms of error was used to simulate uncertainties in depth over a 15 m range that groupers are commonly found. WGN ranging from 0 to 30 dB was added to each of these arrivals. Prior to beginning the localization method, receiver arrivals were discarded at a probability rate representative of the percentage of usable arrivals at each receiver for actual Nassau grouper sounds: 79, 68, 58, 90, 100, and 80% for receivers 1 to

6 were respectively. A 2D, 5 m gridded area was used with 500 simulations per position.

In addition to these simulations, the 22 kHz pings produced at known locations were used to approximate error using real data that inherently have uncertainties not simulated such as recorder synchronization, receiver positions, and acoustic propagation. The pings were manually detected in the recordings and bandpass filtered between 21 and 23 kHz using an FIR filter. The TDOAs between pings were measured using cross correlation. To reduce errors due to the surface reflections, the median TDOA measured for each pair of receivers was used for hyperbolic localization. The mean and standard deviation of error for all 15 positions were calculated and these empirical measurements were used to determine which simulation best represented the true localization error.

D. Grouper call localization & source levels

All the data from receiver 5 was visually examined for sounds produced by four grouper species and the call type and the start and end times of each sound were recorded. These calls were then passed through the localization method described above to produce a 2D position estimate and a residual error. Any positions with residual error greater than 0.0001 m or outside the 6.4 km^2 area used for simulations were discarded.

For each call type, the 200 localized sounds with the lowest residual error for position estimates were used to measure the RMS and peak-to-peak (PP) received level (RL) of call arrivals. RMS measurements were made over 5 to 95% of the energy using the recorded start and end times. The arrivals of these sounds were band-pass filtered (Table 1) and the arrival with the greatest SNR or with the lowest interference was used to measure RL. Spherical spreading was assumed for transmission loss (TL) since water depth was comparable to the distance across the array. Given this information and the distance, *D*, between the receiver of the selected arrival and location where the sound was produced, the RMS and PP source level (SL) can be estimated (3).

$$SL = RL + 20\log D \quad (3)$$

III. Results

Over 45,000 manually detected sounds were passed through the match filtering and SNR analysis to create a subset of high quality calls for localization. More than 26,000 calls were localized, providing continuous observation of Nassau grouper and red hind spawning aggregation activity and movements within the array for over a week.

A. 2D localization error

The empirical error measurements and error simulations produced a range of results that likely represent both the best and worst cases for localization. The 3D simulation for testing the NLLS algorithm error indicated that the error in 2D position at 30 m depth was 0 m both inside and outside the array. Over a 15 m depth range from 20 to 35 m, the error was less than 0.2 m at the center of the array and increased to about 3 m near the perimeter with a mean error for these depths of 1.1 ± 1.7 m across the 6.4 km^2 area. The 2D error related to TDOA measurement error ranged from < 2 m near the center to approximately 7 m near the perimeter for the TDOA error between ± 4 ms and closer to 7 m error across all of the array for TDOA errors between ± 14 ms (Fig. 2). The final simulation, which was designed to most closely resemble grouper sound and localizations, ranged from approximately 4 to 20 m error from the center to the perimeter. The mean position error was 16.6 ± 0.9 m inside the array and 36.2 ± 0.9 m outside for the 6.4 km^2 area (Fig. 3).

The position estimates for the known pinger locations had errors that ranged from 0.08 m at receiver 3 to 11 m at 10 m outside receiver 5 (Table 2). The mean error for these 15 known

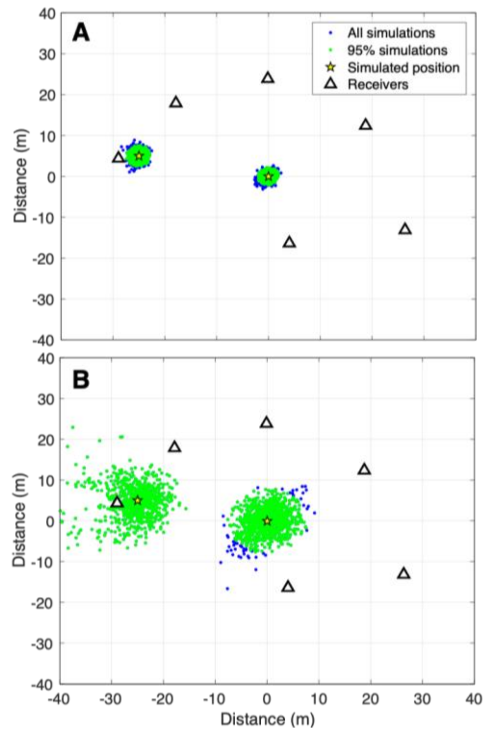

Fig. 2. Example simulations for a position near the center of the array and the perimeter for TDOA error measurements between A) ± 4 ms and B) ± 14 ms. The simulated positions are indicated by the stars with triangles marking receiver locations. Circles show the localization results for 1000 simulations in blue with the 95% percentile shown in green.

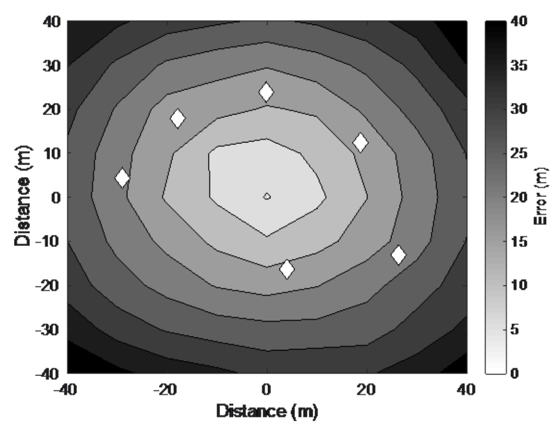

Fig. 3. Localization error for the 2D area of the array and the SNR simulation. Contours were created from error estimates at positions separated by 5 m across an 80 m x 80 m area containing the array. Receiver locations are marked by white triangles and the colored contours represent position errors ranging from ~5 m for lighter colors to 45 m for darker colors.

TABLE II. EMPIRICAL LOCALIZATION ERROR. The known sound source locations are indicated in the first column by the receiver number with the distance in or out of the array if applicable. For each, the difference between the known location and the localized position is shown for the x-axis (Error X), y-axis (Error Y), and the Euclidean difference (Total Error).

Position	Error X (m)	Error Y (m)	Total Error (m)
1	-0.31	-0.26	0.40
2	5.73	-1.82	6.01
3	0.08	-0.02	0.08
4	0.33	-1.31	1.35
5	-0.11	-0.24	0.26
6	5.77	-1.53	5.97
1- 5 m in	0.63	0.62	0.88
2- 5 m in	-0.19	0.22	0.29
3- 5 m in	-0.04	0.74	0.74
4- 5 m in	-0.04	0.51	0.51
5- 5 m in	-0.21	-0.13	0.25
6- 5 m in	0.66	0.34	0.74
1- 5 m out	-3.17	3.23	4.53
3- 5 m out	1.02	1.1	1.50
5- 5 m out	-0.12	-5.63	5.63
1- 10 m out	-9.22	5.64	10.81
3- 10 m out	7.75	1.21	7.84
5- 10 m out	-0.66	-11.02	11.04

locations was 3.27 ± 3.75 (m) for positions inside and outside the array and 1.46 ± 2.15 m for inside the array only. By combining the localization simulations and estimates of known sound source positions, we estimate that the position error for 20 to 35 m depth was approximately 2-5 m near the center of the array, 7-15 m around the perimeter, and higher error outside of the array.

B. *Grouper localizations*

Of the 26,000 localized sounds, the majority were produced by Nassau grouper and red hind (Table 3). Calls indicated two areas of increased calling activity during peak calling days; both areas were located in sandy bottoms between coral formations. During the hour around sunset, approximately 17:30 to 18:30, there were very few localized calls by Nassau grouper (Fig. 4A), which corresponded with times when spawning was observed

TABLE III. TOTAL GROUPER SOUNDS AND LOCALIZATIONS. For each species listed in the first column, the total number of sounds manually detected on the reference receiver are shown in the second column (No. of sounds) along with the number of sounds that met the criteria for localization in the third column (No. of localized sounds) and the number of localizations that were discarded due to residual error or the location being outside the defined 80 x 80 m area (No. of discarded positions).

Species	No. of sounds	No. of localized sounds	No. of discarded positions
Nassau	16,898	15,633	2,848
Red hind	27,565	18,081	4,761
Black	1,351	943	251
Yellowfin	431	226	75

outside of the array (along the shelf break). Localizations indicated movements of Nassau grouper in and out of the array, suggesting possible movements to and from spawning.

Localizations of red hind calls over the duration of the deployment indicated high call activity in three areas within the array (Fig. 4B). In comparison to Nassau grouper, more red hind calls occurred in the southwest corner of the array between receivers 2 and 3. These calls extended outside the array into deeper areas between 30 and 40 m depth. The highest number of localized calls occurred between 17:00 to 18:00, when Nassau grouper calls were least common (Fig. 4B). For a couple of hours following sunrise, approximately 6:30 to 8:30, few red hind calls were localized in the study area (Fig. 4B).

C. *Source levels*

The mean peak-to-peak source levels of calls ranged from 143.7 ± 6.4 dB for yellowfin grouper to 154.9 ± 5.1 dB for Nassau grouper (both re: 1μPa at 1m over 70 to 170 Hz) (Table 4). Given the mean SLs and a reasonable shallow water ambient noise condition of 90 dB re 1 μPa [36], assuming spherical spreading and no bottom effects, the upper bound for the detection range is estimated to be between 0.3 to 1 km. Using the mean distance between the receivers and the calls used for SL measurements, 34.6 ±13.1 m, and localization error for the ground-truth locations inside and outside the array, we calculated that the source level estimate error caused by

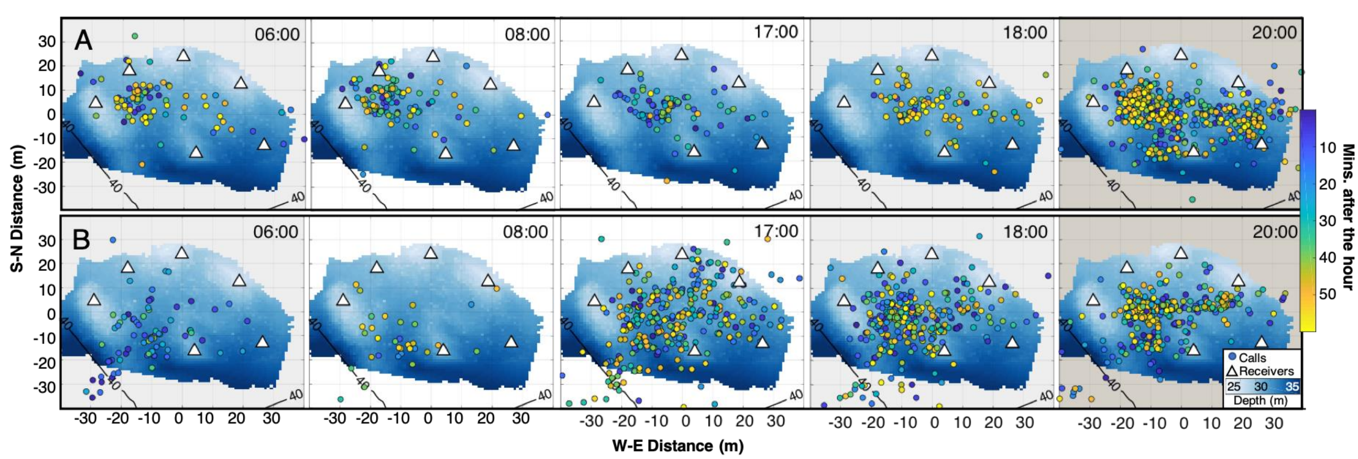

Fig. 4. Five hours of A) localized Nassau grouper sounds during a spawning day, February 15 and B) localized red hind sounds on the day with the highest sound occurrence, February 18. One hour of sound localizations, beginning at the time indicated in the top-right, are shown in each panel. Blue-to-yellow gradient indicates when, following the starting time, sound was produced. The background color of each panel reflects either nighttime (dark grey), hour of sunrise or sunset (light grey), or daytime (white). Triangles indicate receiver locations. Water depth varies from 25 m (white) to 35 m (dark blue).

TABLE IV. GROUPER SOURCE LEVELS. The mean peak-to-peak (SL_{pp}) and RMS (SL_{rms}) source levels for each species listed in the first column are presented with the standard deviation in column two and four, respectively. The full range of measurements for each of these source levels is shown in the columns that follow each, column three (SL_{pp} range) and four (SL_{rms} range). Lastly, the total number of source level measurements made for each species is indicated in the last column.

Species	**Peak-to-peak source level (SL_{pp}) (dB re 1μPa @ 1m)**	**SL_{pp} range**	**RMS source level (SL_{rms}) (dB re 1μPa @ 1m)**	**SL_{rms} range**	**Sample size**
Nassau	152.0 ± 6.5	121.9 - 167.4	137.9 ± 6.4	105.9 - 154.3	751
Red hind	146.8 ± 5.2	129.8 - 162.7	132.6 ± 5.6	116.1 - 150.6	345
Black	150.3 ± 5.3	128.1 - 165.4	135.0 ± 5.6	113.6 - 151.4	159
Yellowfin	143.7 ± 6.4	122.3 - 157.1	127.4 ± 6.5	105.4 - 141.9	133

positioning error could be from 2.3 dB at the center to 10.4 dB (re 1 μPa) near the array perimeter.

IV. DISCUSSION

A passive acoustic localization method was developed, evaluated, and applied to calls recorded during the spawning of Nassau grouper enabling continuous observation of a Nassau grouper FSA and a possible red hind aggregation. In addition, we obtained the first measurements of source levels for these species, as well as black and yellowfin grouper. Localization of grouper calls was challenging due to high levels of variable and impulsive noise in the shallow-water environment, biological sounds that could cause interference, and the need to synchronize instruments with fine accuracy and precision (<0.1 ms) due to the smaller spatial ranges of sound propagation for these fishes.

The accuracy of localization is impacted by the above factors as well as the uncertainty in receiver positions, environmental properties (sound speed, bottom type, etc.) and propagation effects, and the number of arrivals used for localization. The currents around Little Cayman are complex, variable, and can be strong [37, 38] and these currents, along with tides, can produce flow and strumming noise in passive acoustic recordings. Some of our receivers (particularly 2 and 3) were more prone to this latter type of noise due to their location and proximity to the shelf edge. Because of this, many of the sounds we localized only had three or four usable arrivals.

The localization error was investigated through empirical measurements and simulations. The collection of ground-truth data to verify the array geometry and methods was critical for developing reliable, robust localization methods and estimating the localization error. This is highly recommended for all future passive acoustic localization studies.

The empirical measurements and simulations had indicated localization errors of 5 to 15 m within the array. We estimated this could contribute 2.3 to 10.4 dB error to SL measurements. However, many calls were localized inside the array compared to the perimeter, thus, source level error is expected to be closer to 2 dB for this set of measurements.

Only 2D localization was achieved for this study due to insufficient depth aperture on our array and only 3 or 4 usable arrivals for a majority of the sounds. However, 3D localization could improve the accuracy and precision of positions and SL measurements. Use of additional receivers, receivers at different depths across the water column, and preliminary tests to determine the best deployment configuration to reduce noise at each hydrophone would make 3D localization achievable.

These were the first measurements of source levels for the family Epinephelidae. The measured grouper source levels fell within the range of previously reported fish source levels [8]–[15]. The measured source levels were also comparable to maximum received levels reported for these grouper sounds in other studies [26]-[30].

Results and the localization methods developed in this study can allow estimates of data necessary to develop density estimation methods, such as source levels and detection probabilities. Similar observations can also be used to further assess how these animals and other sound-producing fish are using their habitats, and to evaluate their acoustic space, which can guide management of sound-producing species.

Further information on the spatial area of grouper spawning aggregations in Little Cayman, call production rates, density estimates, and communication and detections ranges of spawning aggregations would enable fisheries managers to better assess and develop management strategies and could help contribute to adaptive management solutions. Additionally, studies using localizations can be extended to address many of the remaining questions about fish acoustic communication, fish bioacoustics, and spawning ecology. For example, further analysis of Nassau grouper and red hind localizations to possibly isolate individuals who are simultaneously calling and moving within the aggregation would enable measurements of call production rate and swimming speed for these species. The first, call production rate, is one of the pieces of information necessary for estimating cue rates, which would contribute to fish abundance estimation using passive acoustics [7].

ACKNOWLEDGMENT

We thank C. Schurgers, J. Jaffe, and R. Kastner for their support as co-principal investigators under the NSF grant, the Cayman Island Department of Environment for their collaboration and support of field work, all the REEF and Grouper Moon volunteers who also supported field work, P. Naughton for his assistance with creating the bathymetry map, and W. Hodgkiss and J. Hildebrand for their assistance in signal processing and localization.

REFERENCES

[1] D. A. Mann, "Acoustic Communication in Fishes and Potential Effects of Noise," The Effects of Noise on Aquatic Life II, Springer, New York, NY, pp. 673–678, 2016.

[2] Y. Sadovy de Mitcheson, “Mainstreaming Fish Spawning Aggregations into Fishery Management Calls for a Precautionary Approach,” BioScience, vol. 66(4), pp. 295–306, 2016.

[3] W. C. Cummings and D. V. Holliday, “Passive acoustic location of bowhead whales in a population census off Point Barrow,” Alaska. J Acoust Soc Am, vol. 78(4), pp. 1163–1169, 1985.

[4] L. E. Freitag and P. L. Tyack, “Passive acoustic localization of the Atlantic bottlenose dolphin using whistles and echolocation clicks,” The Journal of the Acoustical Society of America, vol. 93(4), pp. 2197–2205, 1993.

[5] J. Gedamke, D. P. Costa, and A. Dunstan, “Localization and visual verification of a complex minke whale vocalization,” The Journal of the Acoustical Society of America, vol. 109(6), pp. 3038–3047, 2001.

[6] Y. Simard, M. Bahoura, and N. Roy, “Acoustic detection and localization of whales in Bay of Fundy and St. Lawrence Estuary critical habitats,” Canadian Acoustics, vol. 32(2), pp. 1–10, 2004.

[7] T. A. Marques, L. Thomas, J. Ward, N. DiMarzio, and P. L. Tyack, “Estimating cetacean population density using fixed passive acoustic sensors: An example with Blainville’s beaked whales,” The Journal of the Acoustical Society of America, vol. 125(4), pp. 1982–1994, 2009.

[8] J. V Locascio and D. A. Mann, “Localization and source level estimates of black drum (Pogonias cromis) calls,” The Journal of the Acoustical Society of America, vol. 130(4), pp. 1868–1879, 2011.

[9] J. F. Barimo and M. L. Fine, “Relationship of swim-bladder shape to the directionality pattern of underwater sound in the oyster toadfish,” Canadian Journal of Zoology, vol. 76(1), pp. 134–143, 1998.

[10] K. Lindström and M. Lugli, “A Quantitative Analysis of the Courtship Acoustic Behaviour and Sound Patterning in Male Sand Goby, *Pomatoschistus minutus,”* Environmental Biology of Fishes, vol. 58(4), pp. 411–424, 2000.

[11] M. W. Sprague and J. J. Luczkovich, “Measurement of an individual silver perch Bairdiella chrysoura sound pressure level in a field recording,” The Journal of the Acoustical Society of America, vol. 116(5), pp. 3186–3191, 2004.

[12] A. Širović, G. Cutter, L. Butler, and D. Demer, “Rockfish sounds and their potential use for population monitoring in the Southern California Bight,” ICES Journal of Marine Science, vol. 66(6), pp. 981–990, 2009.

[13] M. J. G. Parsons, S. Longbottom, P. Lewis, R. D. McCauley, and D. V. Fairclough, “Sound production by the West Australian dhufish (Glaucosoma hebraicum),” The Journal of the Acoustical Society of America, vol. 134(4), pp. 2701–2709, 2013.

[14] D. E. Holt and C. E. Johnston, “Sound production and associated behaviours in blacktail shiner Cyprinella venusta: a comparison between field and lab,” Environmental Biology of Fishes, vol. 97(11), pp. 1207–1219, 2014.

[15] B. E. Erisman and T. J. Rowell, “A sound worth saving: acoustic characteristics of a massive fish spawning aggregation,” Biology letters, vol. 13(12), 2017.

[16] T. J. Rowell, D. A. Demer, O. Aburto-Oropeza, J. J. Cota-Nieto, J. R. Hyde, and B. E. Erisman, “Estimating fish abundance at spawning aggregations from courtship sound levels,” Scientific Reports, vol. 7(1), pp. 3340, 2017.

[17] T. J. Rowell, M. T. Schärer, R. S. Appeldoorn, M. I. Nemeth, D. A. Mann, and J. A. Rivera, “Sound production as an indicator of red hind density at a spawning aggregation,” Marine Ecology Progress Series, vol. 462, pp. 241–250, 2012.

[18] V. M. Janik, “Whistle matching in wild bottlenose dolphins (Tursiops truncatus),” Science, vol. 289(5483), pp. 1355–1357, 2000.

[19] R. Morrissey, J. Ward, N. Dimarzio, S. Jarvis, and D. Moretti, “Passive acoustic detection and localization of sperm whales (Physeter macrocephalus) in the tongue of the ocean,” Applied Acoustics, vol. 67, pp. 1091–1105, 2006.

[20] S. Kay, Fundamentals of statistical signal processing: Detection theory, 1998.

[21] J. L. Spiesberger and K. M. Fristrup, “Passive Localization of Calling Animals and Sensing of their Acoustic Environment Using Acoustic Tomography,” The American Naturalist, vol. 135(1), pp. 107, 1990.

[22] G. C. Carter, “Coherence and time delay estimation,” Proceedings of the IEEE, 1987.

[23] I. Céspedes, J. Ophir, and S. K. Alam, “The combined effect of signal decorrelation and random noise on the variance of time delay estimation,” IEEE Transactions on Ultrasonics, Ferroelectrics, and Frequency Control, 1997.

[24] M. Azaria and D. Hertz, “Time Delay Estimation by Generalized Cross Correlation Methods,” IEEE Transactions on Acoustics, Speech, and Signal Processing, 1984.

[25] S. M. Wiggins, K. E. Frasier, E. Henderson, and J. A. Hildebrand, “Tracking dolphin whistles using an autonomous acoustic recorder array,” The Journal of the Acoustical Society of America, vol. 133(6), pp. 3813–3818, 2013.

[26] T. Rowell, M. Schärer, and R. Appeldoorn, “Description of a new sound produced by Nassau grouper at spawning aggregation sites,” Gulf and Caribbean Research, vol. 29, pp. GCFI 22–26, 2018.

[27] M. T. Schärer, T. J. Rowell, M. I. Nemeth, and R. S. Appeldoorn, “Sound production associated with reproductive behavior of Nassau grouper Epinephelus striatus at spawning aggregations,” Endangered Species Research, vol. 19(1), pp. 29–38, 2013.

[28] M. T. Schärer, M. I. Nemeth, D. Mann, J. Locascio, R. S. Appeldoorn, and T. J. Rowell, “Sound production and reproductive behavior of yellowfin grouper, Mycteroperca venenosa (Serranidae) at a spawning aggregation,” Copeia, vol. 1(1), pp. 135–144, 2012.

[29] M. T. Schärer, M. I. Nemeth, T. J. Rowell, and R. S. Appeldoorn, “Sounds associated with the reproductive behavior of the black grouper (Mycteroperca bonaci),” Marine Biology, vol. 161(1), pp. 141–147.

[30] D. Mann, J. Locascio, M. Schärer, M. Nemeth, and R. Appeldoorn, “Sound production by red hind epinephelus guttatus in spatially segregated spawning aggregations,” Aquatic Biology, vol. 10(2), pp. 149–154, 2010.

[31] V. Banzon, T. M. Smith, C. Liu, and W. Hankins, “A long-term record of blended satellite and in situ sea surface temperature for climate monitoring, modeling and environmental studies,” Earth System Science Data Discussions, 2016.

[32] E. P. Chassignet, H. E. Hurlburt, O. M. Smedstad, G. R. Halliwell, P. J. Hogan, A. J. Wallcraft, R. Baraille, and R. Bleck, “The HYCOM (HYbrid Coordinate Ocean Model) data assimilative system,” Journal of Marine Systems, 2007.

[33] T. J. McDougall and P. Barker, “Getting started with TEOS-10 and the Gibbs Seawater (GSW) Oceanographic Toolbox,” Scor/Iapso, vol. Wg127, pp. 28, 2011.

[34] G. L. Turin, “An Introduction to Matched Filters,” IRE Transactions on Information Theory, vol. 6(3), pp. 311–329, 1960.

[35] K.C. Wilson, B.X. Semmens, C. Pattengill-Semmens, C. McCoy, and A. Širović, “Potential for grouper acoustic competition and partitioning at a multispecies spawning site in Little Cayman, Cayman Islands”, unpublished.

[36] R. Urick and W. A. Kuperman. "Ambient noise in the sea," 1989.

[37] R. L. Molinari, M. Spillane, I. Brooks, D. Atwood, and C. Duckett, “Surface currents in the Caribbean Sea as deduced from Lagrangian observations,” Journal of Geophysical Research, vol. 86(C7), pp. 6537, 1981.

[38] L. Whaylen, C. V. Pattengill-Semmens, B. X. Semmens, P. G. Bush, and M. R. Boardman, “Observations of a Nassau grouper, Epinephelus striatus, spawning aggregation site in Little Cayman, Cayman Islands, including multi-species spawning information,” Environmental Biology of Fishes, vol. 70(3), pp. 305–313, 2004.